Prod. Eng. Res. Devel. (2015) 9:179–186
DOI 10.1007/s11740-014-0598-z

PRODUCTION PROCESS

Predicting thermal loading in NC milling processes

Matthias Schweinoch · Raffael Joliet · Petra Kersting

Received: 30 September 2014 / Accepted: 11 December 2014 / Published online: 19 December 2014

Abstract In dry NC milling, a significant amount of heat is introduced into the workpiece due to friction and material deformation in the shear zone. Time-varying contact conditions, relative tool–workpiece movement and continuous geometric change of the workpiece due to material removal lead to a perpetually changing inhomogeneous temperature distribution within the workpiece. This in turn subjects the workpiece to ongoing complex thermomechanical deformations. Machining such a thermally loaded and deformed workpiece to exact specifications may result in unacceptable shape deviations and thermal errors, which become evident only after dissipation of the introduced heat. This paper presents a hybrid simulation system consisting of a geometric multiscale milling simulation and a finite element method kernel for solving problems of linear thermoelasticity. By combination and back-coupling, the described system is capable of accurately modeling heat input, thermal dispersion, transient thermomechanical deformation and resulting thermal errors as they occur in NC milling processes. A prerequisite to accurately predicting thermomechanical errors is the correct simulation of the temperature field within the workpiece during the milling process. Therefore, this paper is subjected to the precise prediction of the transient temperature distribution inside the workpiece.

Keywords Milling simulation · Geometric modeling · Thermal error · Deformation · Process optimization · Finite element method (FEM)

M. Schweinoch (✉) · R. Joliet · P. Kersting
Institute of Machining Technology, TU Dortmund University, Baroper Str. 303, 44227 Dortmund, Germany
e-mail: schweinoch@isf.de

1 Introduction

During machining processes, a significant amount of energy is converted to heat, resulting in a thermally loaded workpiece. Dry NC milling and milling with minimum quantity lubrication are particularly affected by this. Workpieces in a thermally loaded state, which are machined to exact specifications without compensating for thermal effects, may exhibit shape deviations or tolerance violations after unloading. In order to avoid rejects during production, the process must be modified to predict and compensate for thermal error between as-built and designed part.

Compensating thermal errors in any production process postulates that these errors are known, determined either by experimental prototyping or by means of simulating the process to the required level of detail. Simulating thermal errors in NC milling is a challenge due to several aspects. The heat input depends on a number of different process parameters, used materials, tool geometry, and milling strategy. Relative tool–workpiece movement and continuous changes of the workpiece geometry result in time-varying contact conditions. As the tool moves through the workpiece, thermally loaded material is removed while at the same time energy—and hence heat—is introduced into the workpiece. Ongoing geometrical changes affect heat dispersion within the workpiece, while clamping, environmental temperature, and heat transmission coefficient constitute further issues of influence. This results in a complex inhomogeneous and constantly in-flux temperature distribution within the workpiece, which in turn affects the workpiece deformation during the machining process.

In this paper, a hybrid simulation system is presented which, by combination of multiple workpiece models, is capable of accurately predicting transient workpiece

temperatures and deformations during dry NC milling. The system consists of a geometric multiscale process simulation and a fictitious domain finite element method (FEM) kernel. The geometric process simulation is used to advance the state of the milling process with respect to material removal, cutting force calculation, and energy input. This state is then forwarded to the FEM kernel, which updates the thermomechanically induced temperature distribution as well as the resulting displacement field. By back-coupling the displacement field with the geometric process simulation, the resulting thermal errors can be predicted.

In order to attain a correct prediction of shape deviation, the hybrid simulation system must be calibrated with respect to cutting forces and energy input. This can be achieved with simple experiments, which are described in the following. Once calibrated, the accuracy of the workpiece temperature prediction of the hybrid simulation system is validated by comparison with experiments.

2 Related work

Analysis and prediction of thermomechanical shape deviations and thermal errors is an area of ongoing research, with early work dating back to the 1940s [17]. More recently, Davis et al. [3] present an overview of significant findings.

Works on thermoelasticity include classical [6] as well as generalized approaches [2, 8]. Solving problems of thermoelasticity is often attempted with finite element analysis (FEA). It is theoretically possible to predict the chip formation in detail to calculate different contributing factors to thermal loading, like friction and shearing. In practice, model simplifications may result in significant errors, and the application of FEA to complete machining processes is limited by available computing capacity.

Recent research in FEA-based techniques focused on various meshing and material removal techniques [15]. While some models consider only the cutting zone [18], others assume a constant heat input along a predefined cutting path [14]. The first approach allows for an accurate prediction of model stress and temperature in the cutting zone, while the latter allows for the simulation of complete NC programs. Other research considers not only the heat input into the model, but also the partitioning of heat into the tool, workpiece, chip and air [5]. Heisel et al. [7] describe an FE model capable of predicting heat input and thermal distribution in orthogonal cutting.

Various analytical and numerical models have been developed for the prediction of cutting forces, energy input, thermal distribution and induced deformations. An overview of recent advances in the modeling of machining processes can be found in [1]. A well established method for the calculation of cutting forces during NC milling is based on the equation of Kienzle [11], which has found application in a number of simulation systems [4, 16]. By bringing together these areas of research, a prediction of energy input into the workpiece is possible.

It can be stated that the prediction of the chip formation and the heat input depends on a large number of boundary conditions, for which no universal model has yet been found [1]. For this reason, models are usually subject to a specific set of parameters and simplifications. For example, the assumption of some heat input model may depend on the used workpiece material as well as the cutter properties.

The hybrid simulation system described herein is comprised of a geometric process simulation and an *hp*-adaptive FE kernel. The geometric process simulation is used to determine the shape of the workpiece and the uncut chip at some simulation step, as well as the heat input resulting from the performed cutting work. The FE kernel is then utilized to determine the workpiece deformation for that simulation step.

3 Hybrid simulation system

An overview of the hybrid simulation system is presented in Fig. 1. The geometric process simulation makes use of different models in order to efficiently compute process-specific behavior and effects [13]. Among others, the prediction of cutting forces and dynamic behavior is possible. For the purpose of predicting thermal errors, the simulation system was augmented with an energy input model, from which the thermal input can be calculated [9, 19]. Given the thermal input, the workpiece deformation can be determined by standard equations of linear thermoelasticity. These are solved using a fictitious domain FE kernel [10]. After calculating the workpiece deformation, the geometric process simulation can access the deformation at each material point for the current simulation step. By back-coupling the deformation into the process simulation, the thermally induced geometric errors can be modeled.

3.1 Geometric process simulation

The geometric process simulation makes use of constructive solid geometry (CSG) to describe the shape of the workpiece, tool and uncut chip. Even though CSG provides no immediate surface representation, and the primitives are of regular shape, it is particularly well suited for application of Boolean operations and intersection computations. Complex geometries can be represented by sequences or compositions of operations the *union*, *difference* and *intersection*.

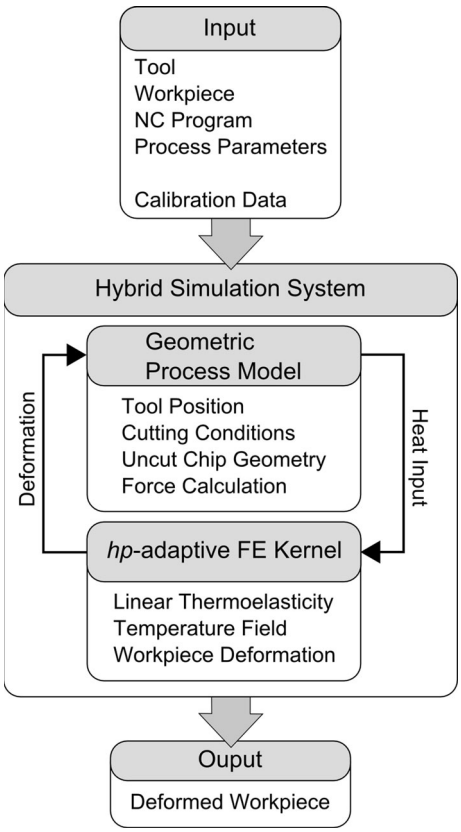

Fig. 1 Overview of the hybrid simulation system

Let W_0 represent the initial CSG shape of the workpiece. Without loss of generality, the workpiece may be considered a stationary object while the tool moves during the process. Let T_i represent the tool shape with applied translation and rotation corresponding to the i-th simulation step. The workpiece geometry at simulation step $i+1$ is then given by $W_{i+1} = W_i \setminus T_{i+1}$. Tool position and rotation are given by the NC file. Hence, the workpiece shape W_n for any simulation step n can be described by the following:

$$W_n = W_0 \setminus \bigcup_{i=0}^{n} T_i. \tag{1}$$

For every simulation step, which corresponds generally to a tooth feed, the shape of the uncut chip can then be described as the intersection of the workpiece geometry and the tool geometry.

$$C_n = W_{n-1} \cap T_n. \tag{2}$$

The uncut-chip thickness is determined by intersection calculations between the uncut-chip geometry and a set of sampling rays. In order to model the sweeping cutting edge of the tool through the workpiece material, each tooth feed is subdivided into a predefinable amount of substeps. For each temporal subdivision of a tooth feed, points on the cutting edge serve as end points of sampling rays that are directed perpendicular to the surface of the rotationally symmetric tool envelope (cf. [12]). Rays in the toroidal part of the cutter are thus generated using a spherical approach, i.e. under consideration of the corner radius. The ray generation is parametric with regard to subdivision of tool axis, circle subdivision, and, for toroidal cutters, spherical sampling.

Given the uncut-chip thickness, the Kienzle equation is used to compute the cutting forces, where specific parameters require calibration by experiment, described in Sect. 4.1. The cutting work can be derived by considering the distance that the cutter moved since the previous simulation step. A heat input model is then used to determine the amount of energy induced into the workpiece [19].

The simulation system is developed in such a way to allow for a substitution or extension of the heat input model. For example, in [9], heat input was uncut-chip-thickness dependent. The current investigation focuses on the comparison of milling strategies. For this contribution, a constant percentage of 23 % of energy was inserted as heat into the workpiece. The used approach modeled the thermal loading of the workpiece to adequate accuracy and was chosen because of its simplicity, although it is by no means universally applicable. Further relevant parameters for the thermal simulation are listed in Table 1.

Table 1 Parameters used for the heat input simulation

Heat transfer coefficient to air	20	$\frac{\mathrm{W}}{\mathrm{m}^2 \cdot \mathrm{K}}$
Heat transfer coefficient to vice	1,800	$\frac{\mathrm{W}}{\mathrm{m}^2\,\mathrm{K}}$
Thermal capacity	862	$\frac{\mathrm{J}}{\mathrm{kg\,K}}$
Material density	2,810	$\frac{\mathrm{kg}}{\mathrm{m}^3}$
Conductivity	115	$\frac{\mathrm{W}}{\mathrm{m\,K}}$

3.2 Thermomechanical finite element model

The linear thermomechanical problem is modeled by means of an *hp*-adaptive FEM that is enriched with a high-order fictitious domain approach [10]. The deformations are discretized via the Crank Nicolson scheme in time, and a higher-order fictitious domain method in space. As the workpiece is subjected to constant geometric changes during the milling process, the FEM meshing scheme is of great importance. A hierarchical mesh of nested hexahedrons with hanging nodes defines the rough shape of the domain and a volume mesh consisting of tetrahedrons, prisms, and pyramids is used in order to describe the boundary of the workpiece.

3.3 Simulation input

Once the simulation system has been calibrated and configured with regard to sampling detail, it requires as input only the process information. Specifically, this includes a CSG description of the workpiece and a parametric description of the tool. The tool is defined by parameters such as diameter, number of teeth, helix angle, and corner radius (in case of a toroidal tool). Furthermore, the actual NC program to be simulated is required as input.

4 Experimental work

The experiments described herein were conducted on a Röders TEC RFM 1000 milling machine. The tools used in the experiments were a FRAISA toroidal cutter AX-R with 1.5 mm corner radius and a FRAISA cylindrical cutter. Both tools have a diameter of 12 mm with two teeth and are made of uncoated HM MG10. The helix angle of the cylindrical cutter is 40°, that of the toroidal cutter 30°.

All probes were made of aluminum AL 7075 T 651, varying in size with respect to the performed experiments.

For thermal measurement, type K thermocouples were fitted into pre-bored holes in the respective probes. Workpiece deformation was measured using multiple Keyence LK-G32 laser sensors in various arrangement. A Kistler 9255 3D force measurement platform was used for force calibration experiments.

4.1 Calibration of force parameters

In order to determine the parameters of the Kienzle equation, a workpiece of dimensions 150 mm × 150 mm × 40 mm (length × width × height) was mounted on a 3D force measurement platform. The workpiece was then machined with varying axial and radial infeed.

The measured forces were used to find optimal parameter values for the Kienzle equation. The calibration procedure was performed for each cutter. Additionally, runout (0.03 mm for the cylindrical and 0.005 mm for the toroidal cutter) of the cutting edges was taken into account. Figure 2 displays a series of tooth engagements for full radial immersion with axial immersion of 2.5 mm.

4.2 Calibration of heat input

The experimental setup for the heat input calibration follows the same principles as described in [9].

Experiments were performed on probes of dimensions 90 mm × 4 mm × 40 mm (length × width × height). Every probe was pre-drilled with small holes on both 4 mm faces.

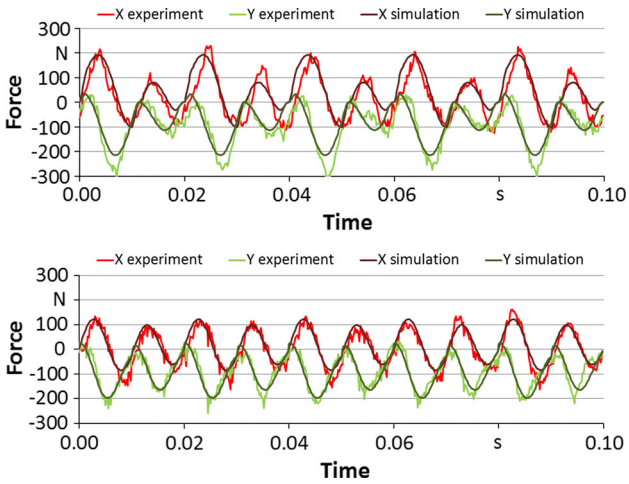

Fig. 2 Calibration of parameter values for the simulation of process forces for the used tools (*top* cylindrical cutter, *bottom* toroidal cutter). Helix angle and runout were taken into account to find suitable force parameters. *Both graphs* present simulated and measured forces in the x direction (*red*) and in the y direction (*green*) (color figure online)

These holes were fitted with type K thermocouples which were offset from the probe base by 5 and 25 mm, respectively.

Every probe was machined to a height of 27 mm. All experiments were performed with parameters $a_p = 1.5\,\text{mm}$, $a_e = 3\,\text{mm}$, $f_z = 0.07\,\text{mm}$, with spindle speed $S = 30,000\,\text{min}^{-1}$.

In comparison to the results described in [9], the simulation underestimates the heat input for the toroidal tool. A crucial simulation parameter apart from the heat input is the thermal flow into the clamping. In previous experiments, workpieces were clamped in polyurethane blocks with low thermal conductivity to prevent a large heat flow into the vice. However, measurements in the polyurethane blocks revealed a temperature increase during the calibration phase, resulting in an error of the simulated heat flow under assumption of a constant boundary temperature. The heat input factor is also very sensitive with respect to the uncut-chip thickness, resulting in great uncertainties of the heat input values for the simulation. In light of these issues, further experiments with an appropriately adapted calibration setup are required to achieve a robust and accurate prediction of heat input for the toroidal tool. Thus, the following results focus on the heat input of the cylindrical tool.

4.3 Comparison of strategies and tools

The validation experiments were performed on probes of dimensions 70 mm × 70 mm × 20 mm (length × width × height). Every probe was pre-drilled with nine holes and fitted with type K thermocouples, as displayed in Fig. 3.

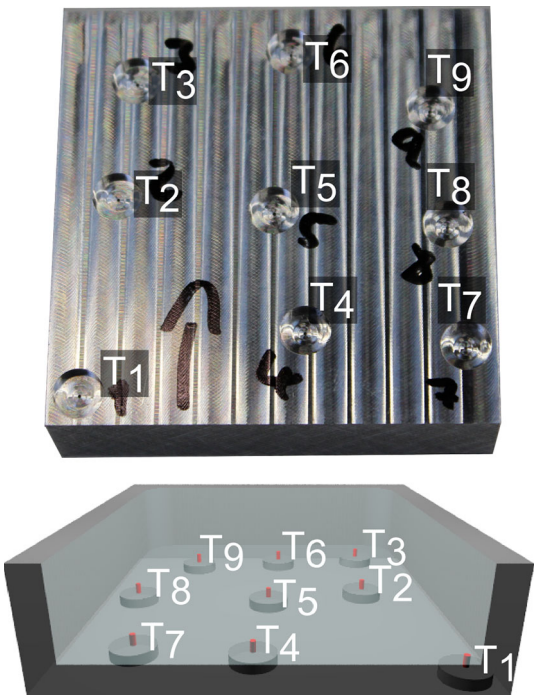

Fig. 3 All workpieces were prepared with inserts for thermocouples on the face opposite to the milling side. Positions were offset from a regular 3×3 pattern to avoid measuring only symmetric data

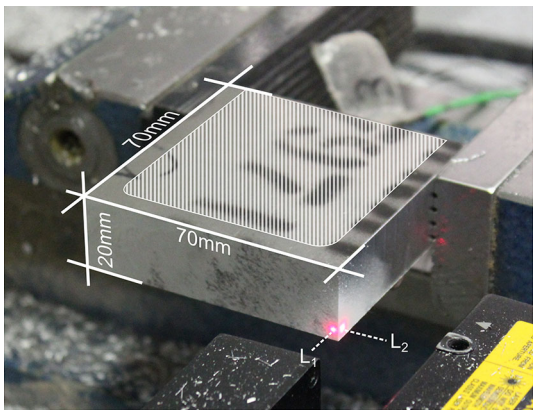

Fig. 4 Experimental setup for strategy and tool analysis with respect to heat input and thermomechanical deformation. The hatched area indicates the location of the cavity. L_1 and L_2 denote the laser sensors used for deformation measurement

The experiments were performed using the same set of parameter values listed in Sect. 4.2.

Deformation was measured in two directions by use of Keyence LK-G32 laser sensors. Probes were clamped excentrically, with a clamping area 20 mm × 20 mm per side, to allow for elongation along one axis. The experimental setup is shown in Fig. 4.

Figure 5 shows the thermal loading of the workpiece for the three strategies that were compared for milling a half-open pocket into the probe: a line-wise strategy (S_1), and two spiraling strategies, where one expands outward from an initial notch (S_2), while the other converges inward in a concentric pattern (S_3).

It should be noted that, for every z level, the initial cut of the strategies S_2 and S_3 requires full immersion of the tool. Subsequently, both strategies continue with $a_e = 3\,\text{mm}$.

5 Results

To provide for clarity, measured and simulated temperatures are only presented for measuring positions T_3 and T_7. Agreeable results between simulation and experiment were observed for the other positions and thus provide no additional insight. The selected positions represent areas of interest with respect to the clamping setup.

The experimental results reveal a large influence of the choice of strategy for pocket milling on the thermal load. Selecting an appropriate strategy is therefor a means of avoiding excessive heat input and reducing the resulting thermomechanical deformations of the workpiece. The duration of the milling process and its intensity, which can be defined by the mechanical load, is of great importance for the overall heating of the workpiece. Furthermore, the varying location of the heat input and the material removal affect the resulting temperature distribution.

Figure 6 displays the workpiece temperature for strategies S_1, S_2 and S_3 at the thermocouples T_3 and T_7, respectively.

Strategies vary with respect to duration of the process and the thermal loading. All strategies revealed a large temperature gradient between the measured locations, with a maximum deviation of up to 10 Celsius at the end of the process. This is due to the heat exchange with the clamping device near T_7 and T_1 (see Figs. 3, 4).

In order to accurately predict thermomechanical deformations of the workpiece, precise measurement and simulation of the temperature distribution within the workpiece is required. The experimental setup allows for an evaluation of the quality of the results obtained by simulation. The heat transfer coefficients from workpiece-to-air and workpiece-to-vice constitute issues of uncertainty. Both values were calibrated together by simulating the cool down of the thermally loaded shape of the workpiece. The temperature increase of the vice in the clamping area is another issue which requires further investigation. By considering a varying vice temperature during the milling process, the boundary conditions for the experiments were determined successfully.

Figures 7, 8 and 9 present a comparison of measured and simulated workpiece temperatures for strategies S_1, S_2 and S_3. These results demonstrate that the simulation

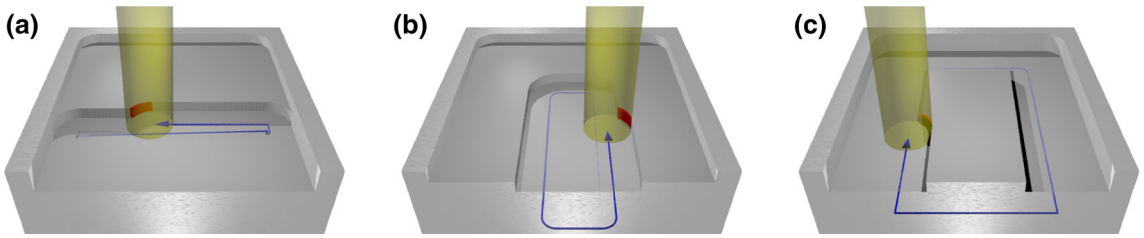

Fig. 5 **a** Strategy S_1: line-by-line milling. **b** Strategy S_2: initial slot milling at the center of the cavity and subsequently outward spiraling tool path. **c** Strategy S_3: initial slot milling along the boundaries of the cavity with subsequently concentric spiraling tool path

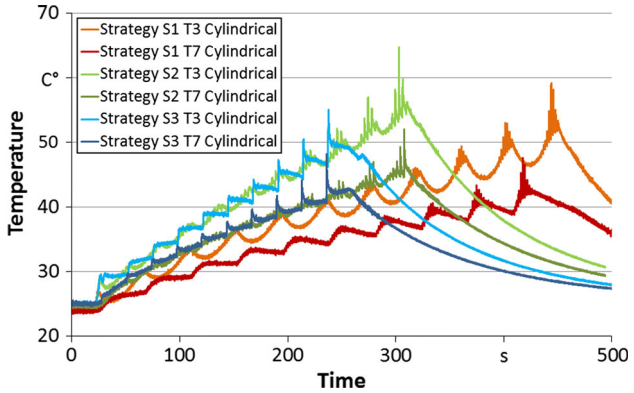

Fig. 6 Comparison of different milling strategies with respect to the thermal loading of the workpiece. Corresponding curves show the measured temperatures at thermocouples T_3 and T_7 for all strategies during the milling process

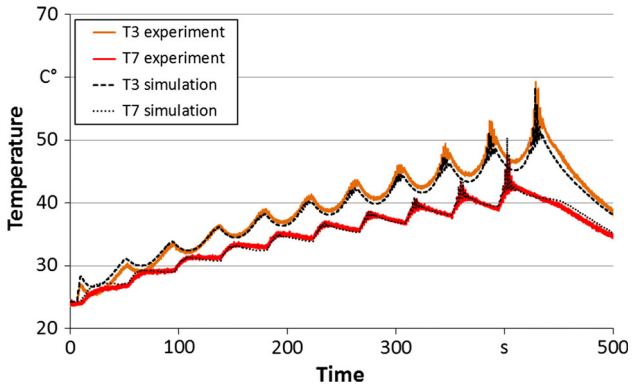

Fig. 7 Comparison of measured and simulated temperatures by example of strategy S_1 using the cylindrical cutter

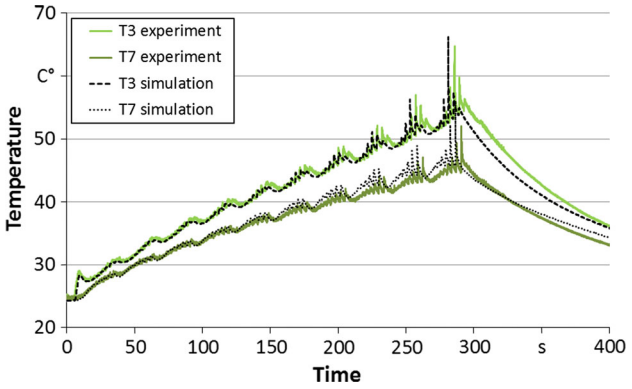

Fig. 8 Comparison of measured and simulated temperatures by example of strategy S_2 using the cylindrical cutter

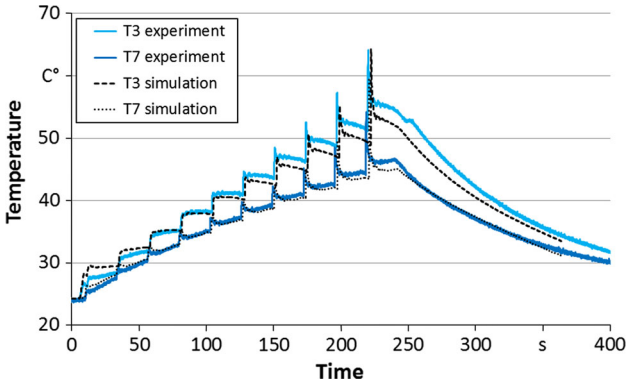

Fig. 9 Comparison of measured and simulated temperatures by example of strategy S_3 using the cylindrical cutter

system is not only able to predict the timing and trend of the workpiece temperature but also its precise level. Small deviations between simulated and measured values can be seen in all diagrams. These may be attributed to measurement errors, model simplifications and thermal effects that were not measured, such as the temperature change of the air around the probe.

The simulations initially outperformed the experiments in terms of process duration. This results from the fact that the simulation is not subject to physical limitations, in particular with respect to acceleration of individual machine axes. As the feed rate of the physical process is not constant throughout, the uncut-chip thickness varies, which in turn results in an overall higher thermal loading of the workpiece when compared with the simulation. For the experiments described herein, the workpiece temperature could be predicted to within acceptable deviations by reducing the feed rate in the virtual process such as to match the duration to the experiment. However, processes of longer duration may not be predictable by such a linearization.

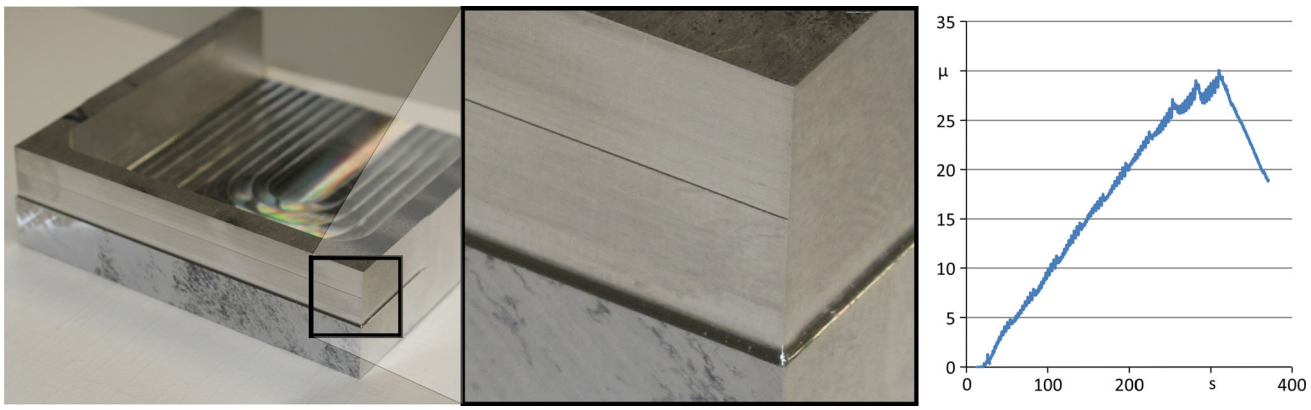

Fig. 10 The displayed probe was machined using strategy S_2. The deformation of the workpiece was ascertained by milling a reference surface prior to milling the cavity, and then milling the same reference surface with reduced a_p. The graph displays the measured thermoelastic deformation of the workpiece in y direction over time

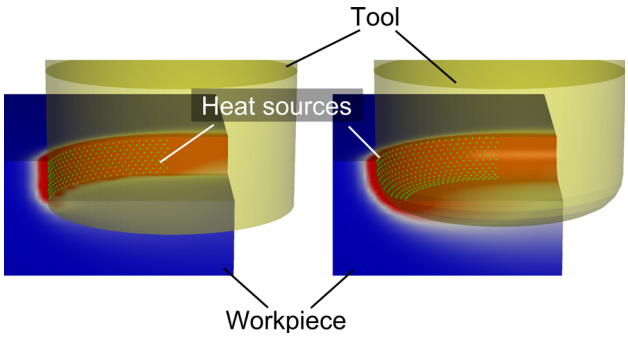

Fig. 11 Simulation of heat input for a cylindrical (*left*) and a toroidal (*right*) cutter. The *green* points denote locations where the thickness of the uncut chip is sampled and a boundary condition (heat source) for the FE simulation is defined. Heat input of the cylindrical tool is predominantly in feed direction. The toroidal tool, due to the corner radius, exhibits a slightly larger heat input into the surface perpendicular to the feed direction (color figure online)

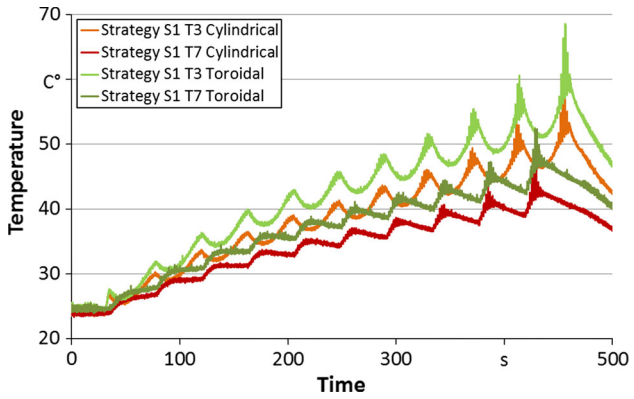

Fig. 12 Comparison of measured temperatures using cylindrical and toroidal cutter for strategy S_1

Figure 10 presents an exemplary result for strategy S_2. The measured thermomechanical deformation in the x and y direction corresponded to the mean temperature difference, as shown in the graph on the right hand side. The visible reference face corresponds to the measured in-process dislocation, allowing for a measurement of deformation after heat dissipation.

Experiments showed that, when all other settings remained unchanged, the toroidal tool resulted in a higher thermal loading of the workpiece than the cylindrical cutter. This can be explained by the different material removal and heat input locations that can be identified in Fig. 11. While the cylindrical tool predominantly induces heat in the feed direction, the toroidal tool, in comparison, also induces a larger amount of heat into the area below the tool. Thermally loaded material in feed direction is removed with the next rotation of the tool, while induced heat below the tool disperses throughout the workpiece.

Figure 12 presents measured temperatures for strategy S_1 for both the toroidal and cylindrical cutter. For the simulation of this effect, calibration of the thickness dependent heat-input factor, as well as the precise modeling of the process forces in the z-direction, is of great importance. These are typically lower than in the other directions, and are primarily caused by the material cutting in the area of the corner radius of the cutter. These effects were not considered within the described simulation system, resulting in a lower thermal input for the toroidal cutter when compared with experimental data.

6 Summary and outlook

The simulation of thermomechanical deformations in dry NC milling requires an accurate prediction of the thermal loading of the workpiece over the course of the process. In this paper experimental and simulation results for a comparison of different strategies for pocket milling were

presented, with the core focus on predicting thermal loading of the workpieces.

A hybrid simulation system was used in order to accurately predict the heat input into the workpiece during complex milling operations. The calculations are based on the Kienzle equation for force computations, calibrated by experiments in order to determine suitable parameter values. By experiment, the different thermal effects of the analyzed strategies could be determined. The simulation was able to model the thermal loading for the cylindrical cutter with a high level of agreement between simulated and measured temperatures over the course of the entire process. Simulation results for the toroidal cutter matched the experimental data in trend, though the overall thermal loading remained below the observed values of the experiments.

Future research will focus on optimizing the simulation system specifically with regards to the following issues: Modeling and calibrating for forces in z-direction with higher accuracy should allow for an accurate simulation of tools with corner radius. Furthermore, correctly modeling the boundary conditions, i.e. changes in temperature in the air about the workpiece, as well as the temperature of the vice in the area of clamping, require further investigation. The simulation system will be extended to allow for a modeling of the physical machine behavior with respect to acceleration of the individual axes. A calibration procedure has to be developed in order to determine workpiece-to-air and workpiece-to-vice heat transfer coefficients.

Transient deformations of the workpieces has been recorded in order to allow for a comparison with simulated deformations. An next step will thus be to verify the hybrid simulation system with respect to predicting workpiece deformation and thermomechanical errors.

Acknowledgments This paper is based on investigations and findings of the project *Simulation of Thermomechanical Deformations in NC Milling* of the priority program SPP 1480 (CutSim) which is kindly supported by the German Research Foundation (DFG).

References

1. Arrazola P, Özel T, Umbrello D, Davies M, Jawahir I (2013) Recent advances in modelling of metal machining processes. CIRP Ann Manuf Technol. doi:10.1016/j.cirp.2013.05.006
2. Bargmann S, Steinmann P (2006) Theoretical and computational aspects of non-classical thermoelasticity. Comput Methods Appl Mech Eng. doi:10.1016/j.cma.2006.05.010
3. Davies M, Ueda T, M'Saoubi R, Mullany B, Cooke A (2007) On the measurement of temperature in material removal processes. CIRP Ann Manuf Technol. doi:10.1016/j.cirp.2007.10.009
4. Denkena B, Böß V (2009) Technological NC simulation for grinding and cutting processes using cuts. In: Proceedings of the 12th CIRP conference on modeling of machining operations
5. Gulpak M, Sölter J, Brinksmeier E (2013) Prediction of shape deviations in face milling of steel. Procedia CIRP. doi:10.1016/j.procir.2013.06.058
6. Haupt P (2002) Continuum mechanics and theory of materials. Transl. from German by Joan A. Kurth., 2nd edn. Springer, Berlin
7. Heisel U, Storchak M, Krivoruchko D (2013) Thermal effects in orthogonal cutting. Prod Eng. doi:10.1007/s11740-013-0451-9
8. Hetnarski RB, Ignaczak J (2000) Nonclassical dynamical thermoelasticity. Int J Solids Struct 37(1–2):215–224
9. Joliet R, Byfut A, Kersting P, Schröder A, Zabel A (2013) Validation of a heat input model for the prediction of thermomechanical deformations during NC milling. In: 14th CIRP conference on modeling of machining operations (CIRP CMMO). doi:10.1016/j.procir.2013.06.124
10. Joliet R, Byfut A, Surmann T, Schröder A (2013) Incremental generation of hierarchical meshes for the thermomechanical simulation of NC-milling processes. In: Eighth CIRP conference on intelligent computation in manufacturing engineering. doi:10.1016/j.procir.2013.09.006
11. Kienzle O (1952) Die Bestimmung von Kräften und Leistungen an spanenden Werkzeugen und Werkzeugmaschinen. VDI-Z 94
12. Odendahl S, Joliet R, Ungemach E, Zabel A, Kersting P, Biermann D (2014) Simulation of the NC milling process for the prediction and prevention of chatter. In: Denkena B (ed) New production technologies in aerospace industry, lecture notes in production engineering. Springer International Publishing, pp 19–25. doi:10.1007/978-3-319-01964-2_3
13. Odendahl S, Kersting P (2013) Higher efficiency modeling of surface location errors by using a multi-scale milling simulation. Procedia CIRP. doi:10.1016/j.procir.2013.06.161
14. Rai JK, Xirouchakis P (2008) FEM-based prediction of workpiece transient temperature distribution and deformations during milling. Int J Adv Manuf Technol. doi:10.1007/s00170-008-1610-6
15. Ratchev S, Nikov S, Moualek I (2004) Material removal simulation of peripheral milling of thin wall low-rigidity structures using FEA. Adv Eng Softw. doi:10.1016/j.advengsoft.2004.06.011
16. Rehling S (2009) Technologische Erweiterung der Simulation von NC-Fertigungsprozessen, Berichte aus dem IFW, Band 01/2009. PZH Produktionstechnisches Zentrum GmbH
17. Schmidt A, Roubik J (1949) Distribution of heat generated in drilling. Trans ASME 71:245–252
18. Smolenicki D, Boos J, Kuster F, Wegener K (2012) Analysis of the chip formation of bainitic steel in drilling processes. In: Fifth CIRP conference on high performance cutting 2012. doi:10.1016/j.procir.2012.05.027
19. Surmann T, Ungemach E, Zabel A, Joliet R, Schröder A (2011) Simulation of the temperature distribution in NC-milled workpieces. Adv Mater Res 223:222–230. doi:10.4028/www.scientific.net/AMR.223.222